Properties of Scalable Distance Minimization Problems using the Manhattan Metric

Heiner Zille
Institute of Knowledge and Language Engineering
University of Magdeburg, Germany
Email: heiner.zille@ovgu.de

Sanaz Mostaghim
Institute of Knowledge and Language Engineering
University of Magdeburg, Germany
Email: sanaz.mostaghim@ovgu.de

***Abstract*—In multi-objective optimization, scalable test problems are required to test and compare the search abilities of the algorithms in solving large and small-dimensional problems. In this paper, we analyze a generalized Distance Minimization Problem (DMP) that is scalable in the number of decision variables and objectives and can be used with any distance function. Since previous research mostly regarded the behaviour of algorithms for Euclidean distances, in this work, we propose to use the Manhattan metric to measure the distances of solutions towards a set of predefined locations in the decision space. The structure of the Pareto-fronts of this problem widely differ from those of the euclidean problem. We perform an analytical analysis exemplary for low-dimensional instances of the problem to provide an understanding of the general properties and structure, and the challenges that might arise in many-objective many-variable instances. The negative effects on the search behaviour of algorithms are theoretically described, and three different optimization methods (MOEA/D, NSGA-II, SMPSO) are tested to give an understanding of different instances of the problem. The experimental results support our expectations and show that the proposed Manhattan metric DMP is difficult to solve for optimization algorithms even in low-dimensional spaces.**

***Keywords*—multi-objective optimization, distance minimization problems, multi-objective test problems, many-objective test problems, scalable test problems**

I. Introduction

In the last years, many-objective and large scale problems have been studied in the area of Evolutionary Multi-objective Optimization (EMO). Such problems provide additional challenges for EMO methods. It is known that by increasing the number of objectives, the performance of the optimization algorithms using Pareto-dominance deteriorates. This is due to the large number of non-dominated solutions in the population [1], [2]. For evaluating the performance of EMO algorithms, scalable test problems have been introduced. Some of them like ZDT-problems [3] are scalable in terms of the number of variables while others like the DTLZ [4] or WFG [5] are scalable both in terms of the number of variables and objectives. One challenge in evaluating the solutions of these problems for large number of objectives concerns the visualization of the results.

Recently Distance Minimization Problems (DMP) are being introduced as scalable test problems which can be easily visualized in the objective space. This kind of problem contains several predefined objective points (the same as the number of objectives) in the decision space. The goal is to find the solutions in the decision space which have the minimum Euclidian distances to all of the objective points. In the previous research this problem was mostly used to visually demonstrate certain search behaviour of algorithms. A basic version of the Distance Minimization Problem was introduced in [6] and [7] and has been reformulated in other research since then. Schütze et al. used quadratic Euclidian distances to obtain a convex optimization problem for their analytical analysis and showed that an increase in the number of objectives does not significantly increase the hardness of an optimization problem [8]. In their work they first formulated the problem for arbitrary numbers of variables and objectives.

Different versions of the DMP, sometimes also with multiple Pareto-optimal areas, were used in [9], [10], [1] and [11]. In [10], an instance of a DMP was created from a real-world map to determine optimal living positions within a city, using the Euclidean metric as an approximation of the distances within the map. In [1] Ishibuchi et al. used the DMP to visually examine the search behaviour of algorithms and applied existing algorithms such as NSGA II, SPEA2 and MOEA/D to problem instances of 2 and 4 objectives with up to 1000 variables. They found that the increase in the number of decision variables had a negative effect on the diversity of solutions, and showed that the solutions converged towards the Pareto-front with a low diversity and spreading out more along the front once it was reached. This research was extended in [11] to 6- and 8-objective instances, and showed that an increase in the number of decision variables has a large influence on solution quality compared to the increase in the number of objectives.

However, all previous studies on the Distance Minimization Problem have only considered Euclidean distance measurement, with the exceptions of [8] and [12]. The idea to use different metrics in the distance measurement of this family of problems was initially suggested in [12], but didn't provide detailed analysis of the specific properties of the problem when using Manhattan-distances. When using only Euclidean distances, the Pareto-fronts consist of one or more convex polygons within the decision space. Therefore, in previous work, the problem itself didn't provide a lot of hardness as long as the number of variables was low, and was used mostly for demonstrating search behaviour visually. However in real world applications, the assumption that distances are euclidean might not be a realistic approximation for the actual distances.

978-1-4799-7492-4/15/$31.00 ©2015 IEEE

For instance in logistic applications such as in robot-driven warehousing applications, or grid-like scenarios like street networks, often other measurements are being employed. This leads to the idea to use different distance measurements for the Distance Minimization Problem.

In this work, we generalize this geometric optimization problem that is based on distance minimization. We propose a new optimization problem by using the Manhattan metric for the distance measurement and show various properties and challenges of this problem exemplary on only small instances of the problem. Our proposed generalized DMP will not only be usable for any number of objectives and variables, but also alters its properties and shape of Pareto-fronts depending on the locations and amount of objective-points.

The goal of this paper is to analytically examine the properties of the generalized DMP when using the $p-1$ (Manhattan) metric as a measurement. Our proposed problems properties differ greatly from the existing ones and provide complicated domination structures and hard to find Pareto-fronts already in low-dimensional instances. We want to introduce these properties using a simple 2-variable problem with only 2 and 3 objectives, and demonstrate the difficulties and effects that optimization algorithms have to deal with. We aim to provide a general impression on the structure of the problem, which can be shown by the low-dimensional instances, as a base for further large-scale instances.

The remainder of this paper is structured as follows. First, we give a detailed description of the existing DMP and our proposed generalized form, and analytically examine its properties and challenges. We raise some expectations about the search behaviour of algorithms, mainly when they rely on Pareto-dominance. In the experiments section, we provide some results of 3 popular algorithms (MOEA/D, NSGA-II, SMPSO) and examine their performance mainly with respect to our raised expectations. We want to note here that our focus is not to show advantages of one method over the other, but in general to point out the difficulties that optimization algorithms have to deal with and that might cause them problems in higher dimensional instances of the problem.

II. Problem description

In this section we describe the Distance Minimization Problem (DMP) and its properties. Furthermore, we introduce a special instance of DMP and give a detailed analysis.

The DMP is a scalable multi-objective optimization problem which contains a set of predefined so-called *objective-points* $\{\vec{O}_1, .., \vec{O}_m\}$ with coordinates $\vec{O}_i = (o_{i1}, .., o_{in})^T$ in the n-dimensional decision space. The number of objective-points corresponds to the number of objectives (m). The goal of the DMP is to find a set of solutions vectors ($\in \mathbb{R}^n$) in the decision space which have a minimum distance to all of the objective-points. The general DMP is formulated as follows:

$$\begin{aligned} min \quad & f(\vec{x}) = (f_1(\vec{x}), f_2(\vec{x}), ..., f_m(\vec{x}))^T & \\ s.t. \quad & f_i = dist(\vec{x}, \vec{O}_i) & \forall i = 1, .., m \\ & x_j \leq x_{max} & \forall j = 1, .., n \\ & x_j \geq x_{min} & \forall j = 1, .., n \end{aligned} \tag{1}$$

The central aspect in the DMP is the function for calculating the distance ($dist(\vec{x}, \vec{O}_i)$) between a solution vector $\vec{x}$ and the objective-point $\vec{O}_i$. Most of the previous research has used the Euclidean metric for measuring the distances in the decision space. This metric refers to the naturally shortest distance. It is induced by the $p-2$ norm $\| \vec{a} \|_2 = \sqrt{\sum_{i=1}^{n} |a_i|^2}$ and will therefore also be addressed as the $p-2$ metric in this paper. It gives the distance of two points as:

$$dist_2(\vec{a}, \vec{b}) := \| \vec{a} - \vec{b} \|_2 = \sqrt{\sum_{i=1}^{n} |a_i - b_i|^2} \tag{2}$$

Although this might be the most natural perception of distance, it is not the only one that occurs in applications and theory. In this paper, we use the Manhattan metric (in this paper also called $p-1$ metric), which is induced by the $p-1$ norm, for measuring the distances between two points in the decision space as follows:

$$dist_1(\vec{a}, \vec{b}) := \| \vec{a} - \vec{b} \|_1 = \sum_{i=1}^{n} |a_i - b_i| \tag{3}$$

In the next sections, we illustrate that the $p-1$ metric drastically changes the properties of the DMP and adds to the difficulty of the problem. In the remainder of this paper, we refer to the DMP using the Euclidean ($p-2$) metric as *DMP-2* and the DMP using the Manhattan ($p-1$) metric as the *DMP-1*.

A. Choosing Objective-Points

Finding the positions for the objective-points in the decision space is one of the challenging parts in setting up a DMP problem. Usually they should be evenly distributed in the decision space. In this paper, we set the positions for the objective points $\vec{O}_i$ by using polar-coordinates around a middle point denoted as $\vec{M}$ in the decision space:

$$\begin{aligned} O_i &= g(\vec{A}_i, r, \vec{M}) \\ \vec{A}_i &:= \{\alpha_{i,1}, .., \alpha_{i,n-1}\} \end{aligned} \tag{4}$$

In order to illustrate the features of the DMP, we focus on 2-dimensional decision spaces ($n = 2$) in the following. In this case, we get $\vec{A}_i = \{\alpha_{i,1}\} = \alpha_i$. Therefore the function for obtaining the objective points will reduce to

$$g(\vec{A}_i, r, \vec{M}) = \vec{M} + \begin{pmatrix} r \cdot \cos \alpha_i \\ r \cdot \sin \alpha_i \end{pmatrix} \tag{5}$$

Since we aim to get evenly distributed objective points $\vec{O}_i$ for any number m of objectives, we only need to set the initial value of α_1 and set the remaining values as

$$\alpha_i = \alpha_1 + \frac{(i-1) \cdot 2\pi}{m} \pmod{2\pi} \quad \forall i = 2..m \tag{6}$$

This symmetry will result in symmetrically shaped convex polygons as the Pareto-fronts of the DMP-2, as can be observed in Figure 2. Figure 1 illustrates the positions of

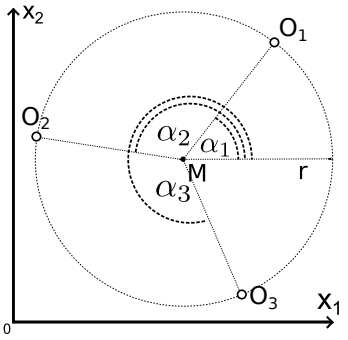

Fig. 1. Example of how to obtain 3 objective points around a central point $\vec{M}$, by defining the three angles α_1, α_2 and α_3

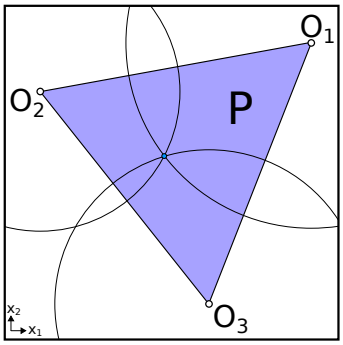

Fig. 2. Decision space of the euclidean DMP for $m = 3$ objectives and $n = 2$ decision variables. The convex triangle (P) is Pareto-optimal. An optimal point is defined by the intersection of distance-circles around the objective-points

three objective-points in a 2-dimensional decision-space. By changing the parameter for α_1 (or in general all the values for $\vec{A}_1 = \{\alpha_{1,1}, .., \alpha_{1,n-1}\}$), we achieve a rotation of the objective-points, which will, as we see in the remainder of the paper, result in drastic changes of the shapes of the Pareto-fronts for the DMP-1.

B. Pareto-fronts of the DMP-2

In order to better understand the overall structure of the problem, we first give a short description of the Pareto-fronts of the DMP-2.

As an example, for the three objective-points $\vec{O}_1$, $\vec{O}_2$ and $\vec{O}_3$ in Figure 2, we see easily that all the solutions that lie within the convex triangle created by the 3 objective-points in the decision space are Pareto-optimal. We can draw the different distance-levels (all solutions with the same distance to one objective-point) as circles around them or in an analytical manner as $\{\vec{s} \in [x_{min}, x_{max}]^2 \ :\| \ \vec{s} - \vec{O}_i \ \|_2 = \ f_i\}$. Each intersection between different minimal circles defines a non-dominated point, and the set of all those solutions form a convex polygon. If we increase the number of objectives or decision variables, the Pareto-optimal solutions for the DMP-2 will always be the set of the convex combinations of all objective-points: $P = \{\vec{s} \mid \vec{s} = \sum_{i=1}^{m} \gamma_i \vec{O}_i \ \wedge \ \sum_{i=1}^{m} \gamma_i = 1 \ \wedge \ \gamma_i > 0 \ \forall i\}$.

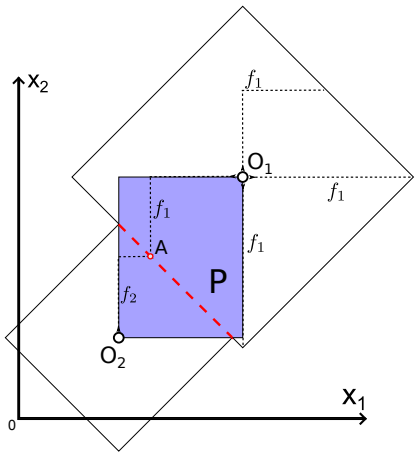

Fig. 3. The Pareto-optimal area between the objective-points $\vec{O}_1$ and $\vec{O}_2$ consists of the intersections of the distance circles. The red dashed line shows the intersection line where all solutions have the same distances to both objective-points as solution A. The whole Pareto-optimal region P is the shaded rectangle composed by all the intersection lines

C. A new Problem: Pareto-fronts of the DMP-1

The Pareto-optimal front in the case of the $p-1$ metric is more complex and has a special structure of dominating solutions compared to the DMP-2.

In Figure 3, we depict the shape of the Pareto-optimal front for 2 objectives in the decision space. For 2 objectives, the entire square defined by the minimum and maximum coordinates of the two objective-points is Pareto-optimal. The distance "circles" from Figure 2 turn to a diamond shape in this case. These diamond shapes define all the points, that have the same distance (measured by the $p-1$ metric) to the respective objective-point in the center. Due to their shape, these "circles" might have more than just one Pareto-optimal intersection point per distance level. This can be seen in Figure 3, where all the solutions that lie on the red dashed diagonal line (as solution A) have the same distances to both objective-points. This means, that there is a large set of Pareto-optimal solutions in the decision space that are all mapped to the same vector in the objective space and are therefore indifferent to each other.

Now we look at the case of more than 2 objectives. We choose 3 objective-points on a circle as described above, and the Pareto-optimal front in the decision space consists of the combination of intersection sets of each two of the objectives. The construction of the Pareto-optimal front is shown in Figure 4. We calculate the Pareto-optimal areas of each pair of the objective-points in the same way as described above, which means we get a rectangular Pareto-optimal front for each pair. For three objective-points $\vec{O}_1, \vec{O}_2$ and $\vec{O}_3$, we obtain the three sets S_{12}, S_{13}, S_{23} of solutions which contain the sets of Pareto-optimal solutions if only the corresponding two objectives are taken into account. Then we construct the intersection sets $I_1 = \{S_{12} \cap S_{13}\}$, $I_2 = \{S_{12} \cap S_{23}\}$, $I_3 = \{S_{13} \cap S_{23}\}$. The union of all these intersection sets form the Pareto-optimal front: $P = I_1 \cup I_2 \cup I_3$.

D. Domination in the DMP-1

For the further analysis, we classify the solutions into different types, which are located in different areas of the decision space. These sets are called type I to IV solutions and are explained in the following. Figure 5 shows an example for the locations of the different types of solutions in a 3-objective scenario.

Type I: Pareto-optimal (bijective objective function) Solution of the types I and II are both part of the Pareto-optimal front of the problem and are therefore globally non-dominated. However, the front consists of two different kinds of solutions. Solutions of type I are unique in a sense that their objective vectors can only be achieved by exactly one combination of decision variables. So the objective function $f(\vec{x})$ is bijective on the set of type I solutions and their objective values. Type I solutions can be found in Figure 5 as lines of solutions in the middle area.

Type II: Pareto-optimal (surjective objective function) Type II solutions are also part of the Pareto-optimal front of the problem. In comparison to type I, solutions of type II are those $\vec{x}$ for which at least there is one other solution $\vec{y} \neq \vec{x}$ with the exact same objective vector: $f(\vec{x}) = f(\vec{y})$. Solutions of type II have actually an infinite number of solutions that have different decision variables but the exact same objective values for every objective. The function $f(\vec{x})$ is therefore surjective but not injective on the set of type II solutions and their objective values. The set of type II solutions forms an area in this problem, as can be seen in Figure 5, and also in the previously explained 2-objective example in Figure 3.

Type III: Dominated by a line Solutions of the types III and IV are not part of the Pareto-optimal front. Type III solution lie within the rectangular area (excluding the type I and II solutions) than is spanned by the minimum and maximum coordinates in each variable j: $o_{j,min} = \min_{i=1..m} o_{ij}$ and $o_{j,max} = \max_{i=1..m} o_{ij}$. Solutions in that area are dominated only by solutions that are located on the exact same line with a gradient of either 1 or -1, and that ends in a Pareto-optimal solution. These dominating lines follow along the intersections of $p-1$ "circles" of two objective points, while the solutions on it can become closer to one other objective, while not leaving the intersection line. Figure 6 illustrates how a type III solution can and cannot be dominated, and Figure 7 depicts how these dominating lines are composed from the $p-1$ "circles" around the 3 objective-points. In this scenario the solution A cannot be dominated easily, even if a solution like D is located very close to the Pareto-front. Unfortunately, the solutions that belong to the same dominating line are the **only** solutions, that dominate their solutions within the entire decision space. If we look at that from another perspective, this implies that even if a Pareto-optimal solution is found, it will dominate only a small subset (of the type III solutions). Such a dominating line is a 1-dimensional set of solutions, which means it has no inner volume. Therefore, a random sampling of the (in theory) continuous decision space would cover the same line two times with a probability of $p = 0$, and therefore dominate a type III solution with a probability of $p = 0$.

Type IV: Dominated by a volume Type IV solutions can be regarded as "easily dominated" solutions. Usually there is a larger set of solutions which can dominate them. In addition, these solutions form a volume, since it is possible to reduce the distance to two or more objective-points at the same time. This means that a randomly chosen solution in the search space can dominate a type IV solution with a probability of $p > 0$. The situation is shown in Figure 8. Type IV solutions are all other solutions that don't belong to the other 3 types, which are in the 3 objective scenario all the solutions outside of the type III rectangle (see again Figure 5.

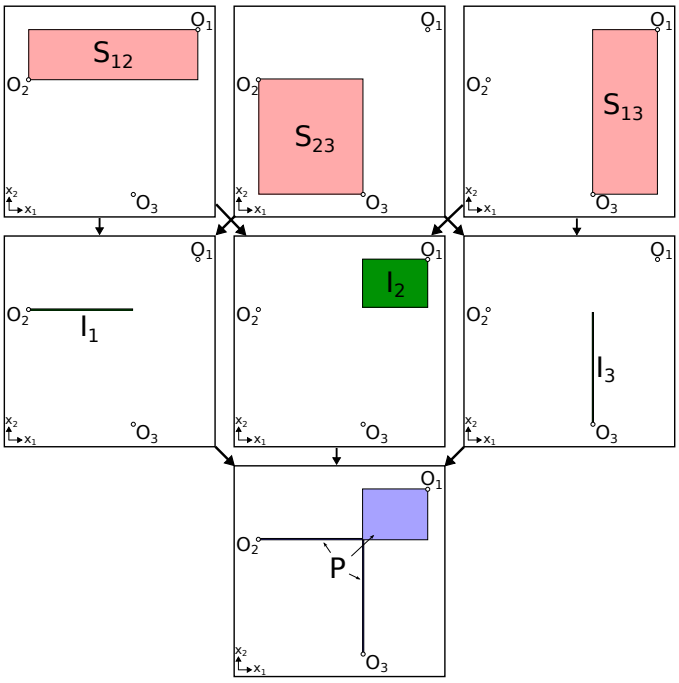

Fig. 4. The Pareto-optimal area (P) of a 3-objective problem is composed by combining the intersection sets (I_1, I_2, I_3) of the different 2-objective optimal areas (S_{12}, S_{13}, S_{23})

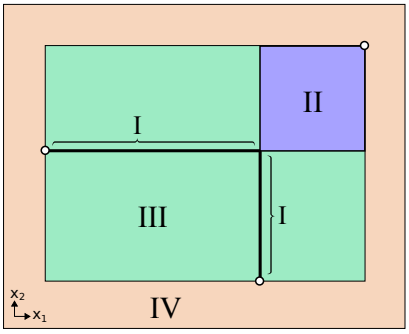

Fig. 5. The locations of the solutions types in a 3-objective problem

E. The Influence of the Offset-Parameter α_1

By creating the objective-points as described above, the initial offset angle α_1 has a strong impact on the shape and properties of the Pareto-fronts. The intersection sets I_i vary from straight lines (type I solutions) only, to a combination of type I and type II volumes. A sketch of the different areas of optimal solutions for 2 and 3 objectives and values of $\alpha_1 = 0, \frac{\pi}{4}$ and $\frac{\pi}{2}$ are illustrated in the Figures 9 and 10.

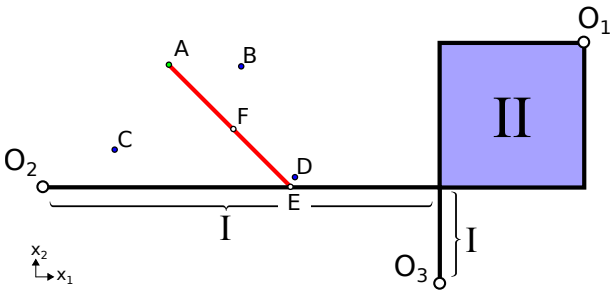

Fig. 6. The Solution A of Type III is only dominated by the solutions E and F, but not by the solutions B, C and D

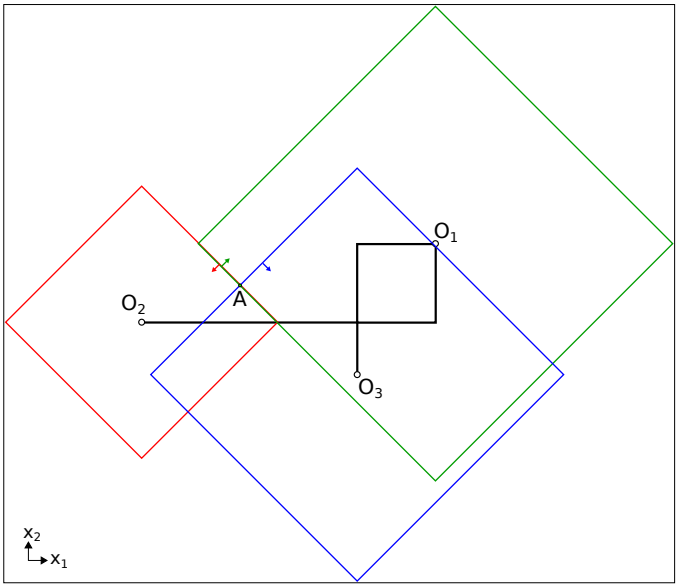

Fig. 7. Intersection of distance-circles in a 3-objective problem. Point A is a type III solution and can move closer to $\vec{O}_3$ while keeping the same distances to $\vec{O}_1$ and $\vec{O}_2$

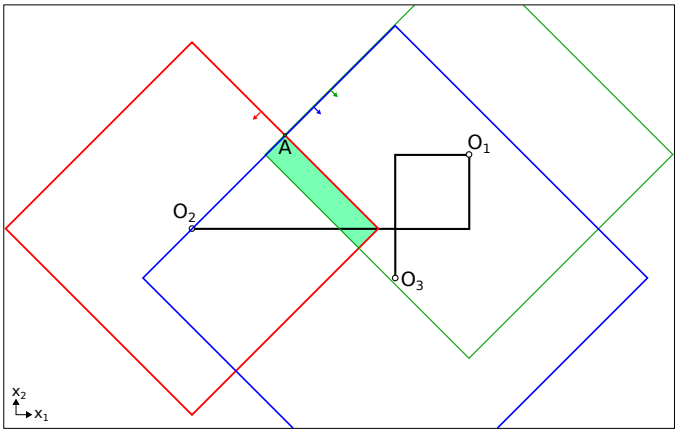

Fig. 8. Intersection of distance-circles in a 3-objective problem. Point A is a type IV solution and is dominated by every solution within the filled rectangular area

In the 2-objective problems, there are no type III solutions. All the solutions inside the rectangle formed by the two objective-points are Pareto-optimal and of type II. This holds for every offset α_1, except when $\alpha_1 = n \cdot \frac{\pi}{2}, n \in \mathbb{N}_0$. In these

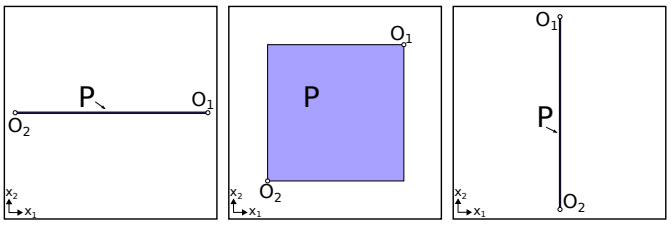

(a) $\alpha_1 = 0$ (b) $\alpha_1 = \pi/4$ (c) $\alpha_1 = \pi/2$

Fig. 9. Example instances of the 2-objective problem and their Pareto-fronts

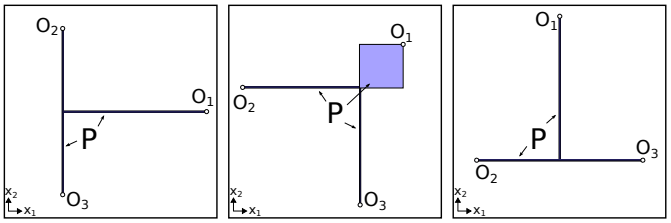

(a) $\alpha_1 = 0$ (b) $\alpha_1 = \pi/4$ (c) $\alpha_1 = \pi/2$

Fig. 10. Example instances of the 3-objective problem and their Pareto-fronts

cases, like seen in the Figures 9a and 9c, the type II area shrinks down to a 1-dimensional line and we only obtain type I solutions as the Pareto-optimal front.

In the 3-objective problems, all 4 kinds of solutions can be found, depending on the offset parameter. In the Figures 10a and 10c, for $\alpha_1 = 0$ or $\alpha_1 = \frac{\pi}{2}$, the Pareto-front consists only of type I solutions, which are surrounded by a square of type III solutions, and type IV solution on the outer sides of the decision space. The most interesting case is shown in Figure 10b. Here, we obtain type IV solutions in the outer decision space and a square of type III solutions formed by the outer boundaries of the objective-points coordinates as described above. The Pareto-optimal front in this problem consists of the type I solutions which form the two lines going up and right inside the space, and a rectangle of type II solutions.

We observe that a variation of the parameter α_1 not only changes the locations and sizes of the Pareto-optimal fronts, but also their types and therefore alter the properties and dominance relations.

F. Problems in the Optimization of the DMP-1

Based on the structure of the Pareto-fronts and the different properties of the solutions for the DMP-1 problem, we expect certain behaviors for the optimization algorithms which use Pareto-dominance. In addition, due to the sparse Pareto-optimal areas in the objective-space, other algorithms such as MOEA/D (which are not based on Pareto-dominance) can also experience some difficulties on this problem.

Expectation 1
Based on the properties of the type IV solutions, we expect that the optimization algorithms can easily find solutions which can dominate a type IV solution (as shown in Figure 8). In addition, such dominating solutions can be found easier, the further the type IV solutions are away from the type III area. *Therefore we expect algorithms to quickly dismiss type IV solutions from the*

population and converge towards the area of type III solutions during the optimization process.

Expectation 2
As type III solutions are only dominated by a very specific set of solutions, namely the ones that lie on the same intersection line between two objectives, it seems improbable for the optimization algorithms (involving randomness) to discover two solutions that lie on the exact same dominating line. Instead, a population of type III solutions is likely to produce more type III solutions surrounding them which will belong to the same non-dominated front. For instance in Figure 6, solution D is not regarded as any "closer" to the Pareto-front as solution A in terms of Pareto-dominance. An evolutionary pressure towards the Pareto-optimal region does hardly exist among type III solutions. *For this reason, we expect algorithms that rely on Pareto-dominance to have slow convergence and difficulties and to approach the Pareto-front from inside the type III areas.*

Expectation 3
Type II solutions form a volume in the decision space which is mapped to a line of Pareto-optimal solutions in the objective-space (since an infinite number of solutions inside that volume maps to the same objective vector). Since most of the optimization methods utilize a clustering in the objective space (and not the decision space), *we expect that, even though there is a clear Pareto-optimal line in the objective space to which an algorithm should converge, the search might result in an unorganized and undesired distribution of solutions throughout type II areas.*

III. Experiments

The goal of our experiments is to provide an impression of the difficulty of the proposed DMP-1 problem and illustrate how existing algorithms deal with this problem. We do not intend to prove one method superior to the others. In addition, we want to raise the questions of how existing algorithms could perform in higher-dimensional instances of the problem.

In our experiments we use the DMP-1 using 2 and 3 objectives and only 2 decision variables like described above. Both problems will be tested with 2 different settings $\alpha_1 = 0$ and $\alpha_1 = \pi/4$, as already seen in the Figures 9a, 9b, 10a and 10b. In the 2-objective problem with $\alpha_1 = 0$ we find only type I and type IV solutions, while the same problem with $\alpha_1 = \pi/4$ only consists of type II and type IV solutions. For the 3-objective instances, the $\alpha_1 = 0$ instance has types I, II and IV solutions, while the $\alpha_1 = \pi/4$ instance has all 4 kinds of solution types to offer. We will set $[x_{min}, x_{max}] = [0, 10]$, $\vec{M} = (5, 5)$ and $r = 2.0$, and let 3 different algorithms solve our problem. These are: MOEA/D ([13]), NSGA-II ([14]) and SMPSO ([15]). The performance of the algorithms is measured by the average number of solutions that are found for each type. Since solutions of type I are numerically hard to find, we apply a tolerance radius of 0.01. Solutions found within this distance of a type I or II solution will be counted as if they actually lied within the desired area.

A. Parameter settings

For the experiments we take the standard values recorded for the algorithms in the literature. The MOEA/D and NSGA-II algorithms use a SBX Crossover ([16]) with a crossover probability of 0.9 and distribution index of 20.0. All 3 algorithms use polynomial mutation ([16]) with a distribution index of 20.0 and a mutation probability of $1/n$. The population size of all three methods is 120. MEOA/D is used without an external archive. For the MOEA/D, the neighbourhood size is 20, the probability of choosing a parent solution from the neighbourhood is 0.9 and the maximum number of replaced solutions for each offspring is 2. All algorithms stop after a fixed number of function evaluations. To be able to examine the convergence of the algorithms, we use three different settings for the number of function evaluations, which are set to 30000, 60000 and 120000, and perform 50 independent runs for each experiment.

B. Results

Tables I to IV show the average number of obtained solutions of each type that are found by the three algorithms for each of the four configurations with 2-, 3-objectives and $\alpha_1 = 0$, $\alpha_1 = \pi/4$. In addition, Figures 11 to 14 illustrate the obtained solutions in the decision space of a selected single run for the four configurations and three tested algorithms. In the following, we analyze the results in terms of the expectations about the search behaviour of the algorithms from the last section.

Expectation 1
According to the results in Tables I to IV, we can conclude that all of the optimization algorithms are able to dismiss type IV solutions from their populations. As there is no type III solution in both of the 2-objective instances, we obtain a good approximation of the Pareto-fronts (although in the $\alpha_1 = \pi/4$ case, the diversity of solutions need to be considered, see below). In addition, we can confirm this visually by looking at the distribution of solutions in the decision space (Figures 11 to 14). All solutions lie within the rectangle ($\alpha_1 = \pi/4$) or line ($\alpha_1 = 0$) defined by the objective points, and are therefore only of the types I, II and III.

Expectation 2
The two algorithms that mainly rely on Pareto-dominance (NSGA-II and SMPSO) fail to approach the actual Pareto-front from within the type III area (Tables III and IV). The results of a single run of the 3 algorithms for both 3-objective instances are shown in the Figures 13 and 14. NSGA-II and SMPSO both rely on Pareto-dominance, and they both suffer from the effects of the hard to dominate type III solutions the most.

In Table III, the MOEA/D algorithm performs slightly better in terms of the obtained type I and II solutions. However, even though it does not rely on Pareto-dominance, it is not showing a good convergence behaviour with increasing number of function evaluations. The increase in found type I and II solutions of the MOEA/D doesn't show a better convergence behaviour than the NSGA-II and SMPSO algorithms, although the overall distribution of solutions seems to lie visually closer to the Pareto-fronts (Figure 13). We see that even though the MOEA/D was able to find slightly more optimal solutions after 30000 evaluations, its convergence seems to be not better than the other methods (Table III).

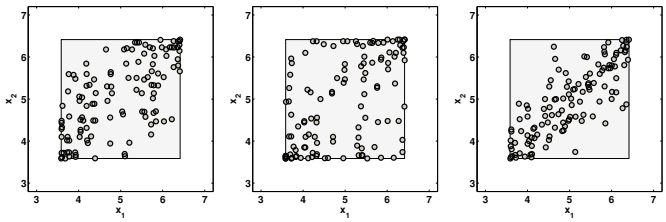

(a) MOEA/D (b) NSGA II (c) SMPSO

Fig. 11. Distribution of solutions of a single run (120000 evaluations) in the decision space (2 objectives, $\alpha_1 = \pi/4$)

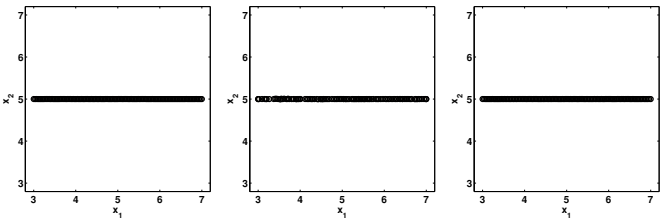

(a) MOEA/D (b) NSGA II (c) SMPSO

Fig. 12. Distribution of solutions of a single run (120000 evaluations) in the decision space (2 objectives, $\alpha_1 = 0$)

A special note goes to the performance of the MOEA/D in the 3-objective $\alpha_1 = 0$ scenario. We observe a superior performance compared to the other two methods (Table IV). This behaviour differs from the performance with the offset of $\pi/4$. We want to denote here that the algorithm performs better in the $\alpha_1 = 0$ scenario because in this special instance of the problem, a part of the Pareto-optimal area of the problem falls together with the connecting line between two of the objective-points. Since the weight vector distribution of the MOEA/D algorithm usually prefers these regions, it is likely that the rather good performance in this $\alpha_1 = 0$ case results from this geometric coincidence. This is supported by Figure 14a, where we see that most of the found Pareto-optimal solutions lie on the connecting line between the two objective-points on the left, but less along the other Pareto-optimal line.

Expectation 3

For our third expectation we take a look at the two Figures 11 and 13. In these instances the Pareto-optimal fronts (partially) consist of type II solutions. In the 2-objective case (Figure 11) the SMPSO shows the best organization of solutions in the type II area, while the MOEA/D and NSGA II obtain a worse organization and the solutions are still distributed widely throughout the area. In the 3 objective case (Table III, Figure 13), we observe that the type II Pareto-optimal areas are on average covered by the NSGA-II and SMPSO slightly less than by the MOEA/D. However, a clear organization of the solutions cannot be seen in our experiments.

In conclusion, we find that in the instances that do not contain type III solutions (both 2-objective instances), all algorithms show a good convergence towards the Pareto-front, even though the distribution of solutions still shows differences in the $\alpha_1 = \pi/4$ scenario. In the 3-objective instances, both algorithms that rely mainly on Pareto-dominance have difficulties to find the Pareto-fronts within the type III solution area, while the MOEA/D can find more optimal solutions already with a low number of function evaluations, but doesn't show much improvement with increasing evaluations.

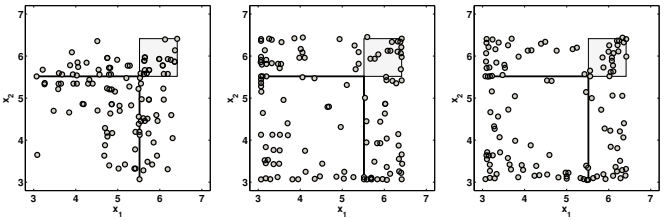

(a) MOEA/D (b) NSGA II (c) SMPSO

Fig. 13. Distribution of solutions of a single run (120000 evaluations) in the decision space (3 objectives, $\alpha_1 = \pi/4$)

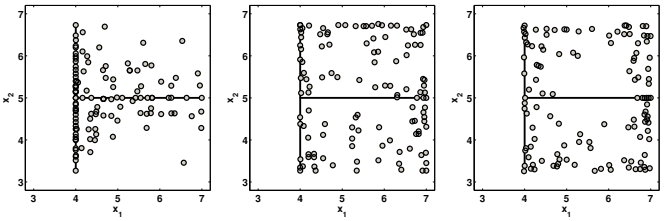

(a) MOEA/D (b) NSGA II (c) SMPSO

Fig. 14. Distribution of solutions of a single run (120000 evaluations) in the decision space (3 objectives, $\alpha_1 = 0$)

TABLE I. AVERAGE NUMBERS AND STANDARD ERRORS (50 RUNS) OF THE DIFFERENT SOLUTION TYPES (2 OBJECTIVES, $\alpha_1 = \pi/4$)

Algorithm	Type I	Type II	Type III	Type IV
30 000 function evaluations				
MOEA/D	—	**119.94** ($\pm$.03)	—	0.06 ($\pm$.03)
NSGA II	—	119.1 ($\pm$.14)	—	0.9 ($\pm$.14)
SMPSO	—	119.62 ($\pm$.07)	—	0.38 ($\pm$.07)
60 000 function evaluations				
MOEA/D	—	**120.0** ($\pm$.00)	—	0.0 ($\pm$.00)
NSGA II	—	118.72 ($\pm$.17)	—	1.28 ($\pm$.17)
SMPSO	—	119.9 ($\pm$.04)	—	0.1 ($\pm$.04)
120 000 function evaluations				
MOEA/D	—	**120.0** ($\pm$.00)	—	0.0 ($\pm$.00)
NSGA II	—	118.72 ($\pm$.18)	—	1.28 ($\pm$.18)
SMPSO	—	**120.0** ($\pm$.00)	—	0.0 ($\pm$.00)

IV. CONCLUSION

In this paper, we proposed a generalization of a m-objective n-variable Distance Minimization Problem, that allows the use of any distance measurement in the decision space. We analytically examined the properties and geometric structure of the problem using the Manhattan metric (p-1) and pointed out the difficulties that arise from that structure. The problem instances used in this paper with only 2 decision variables and only 2- and 3-objectives were used to give an overview of the properties of this scalable test problem and at the same time already provide difficult tasks for optimization algorithms. By our analysis we want to show that the general DMP, using the Manhattan metric, is a difficult optimization problem even with small numbers of dimensions. Since it can be scaled very easily to a many-variable and many-objective problem, it can

TABLE II. AVERAGE NUMBERS AND STANDARD ERRORS (50 RUNS) OF THE DIFFERENT SOLUTION TYPES (2 OBJECTIVES, $\alpha_1 = 0$)

Algorithm	Type I	Type II	Type III	Type IV
30 000 function evaluations				
MOEA/D	**120.0** ($\pm$.00)	—	—	0.0 ($\pm$.00)
NSGA II	119.12 ($\pm$.14)	—	—	0.88 ($\pm$.14)
SMPSO	**120.0** ($\pm$.00)	—	—	0.0 ($\pm$.00)
60 000 function evaluations				
MOEA/D	**120.0** ($\pm$.00)	—	—	0.0 ($\pm$.00)
NSGA II	119.1 ($\pm$.16)	—	—	0.9 ($\pm$.16)
SMPSO	**120.0** ($\pm$.00)	—	—	0.0 ($\pm$.00)
120 000 function evaluations				
MOEA/D	**120.0** ($\pm$.00)	—	—	0.0 ($\pm$.00)
NSGA II	119.34 ($\pm$.16)	—	—	0.66 ($\pm$.16)
SMPSO	**120.0** ($\pm$.00)	—	—	0.0 ($\pm$.00)

TABLE III. AVERAGE NUMBERS AND STANDARD ERRORS (50 RUNS) OF THE DIFFERENT SOLUTION TYPES (3 OBJECTIVES, $\alpha_1 = \pi/4$)

Algorithm	Type I	Type II	Type III	Type IV
30 000 function evaluations				
MOEA/D	**5.82** ($\pm$.39)	**24.9** ($\pm$.25)	88.76 ($\pm$.46)	0.52 ($\pm$.09)
NSGA II	3.8 ($\pm$.18)	15.96 ($\pm$.37)	90.72 ($\pm$.70)	9.52 ($\pm$.51)
SMPSO	2.18 ($\pm$.16)	17.6 ($\pm$.29)	95.44 ($\pm$.37)	4.78 ($\pm$.30)
60 000 function evaluations				
MOEA/D	**6.5** ($\pm$.42)	**25.06** ($\pm$.24)	88.26 ($\pm$.51)	0.18 ($\pm$.06)
NSGA II	3.76 ($\pm$.21)	16.02 ($\pm$.33)	90.24 ($\pm$.72)	9.98 ($\pm$.60)
SMPSO	2.42 ($\pm$.19)	17.92 ($\pm$.28)	95.28 ($\pm$.47)	4.38 ($\pm$.30)
120 000 function evaluations				
MOEA/D	**6.0** ($\pm$.39)	**26.04** ($\pm$.30)	87.94 ($\pm$.49)	0.02 ($\pm$.02)
NSGA II	3.88 ($\pm$.19)	16.36 ($\pm$.32)	87.68 ($\pm$.71)	12.08 ($\pm$.66)
SMPSO	3.14 ($\pm$.16)	18.44 ($\pm$.25)	94.7 ($\pm$.44)	3.72 ($\pm$.28)

TABLE IV. AVERAGE NUMBERS AND STANDARD ERRORS (50 RUNS) OF THE DIFFERENT SOLUTION TYPES (3 OBJECTIVES, $\alpha_1 = 0$)

Algorithm	Type I	Type II	Type III	Type IV
30 000 function evaluations				
MOEA/D	**56.3** ($\pm$.69)	—	63.44 ($\pm$.68)	0.26 ($\pm$.08)
NSGA II	10.52 ($\pm$.38)	—	98.68 ($\pm$.60)	10.8 ($\pm$.56)
SMPSO	9.54 ($\pm$.37)	—	105.56 ($\pm$.37)	4.9 ($\pm$.25)
60 000 function evaluations				
MOEA/D	**59.54** ($\pm$.77)	—	60.44 ($\pm$.77)	0.02 ($\pm$.02)
NSGA II	9.96 ($\pm$.39)	—	98.84 ($\pm$.70)	11.2 ($\pm$.61)
SMPSO	9.62 ($\pm$.38)	—	106.44 ($\pm$.36)	3.94 ($\pm$.24)
120 000 function evaluations				
MOEA/D	**59.44** ($\pm$.82)	—	60.56 ($\pm$.82)	0.0 ($\pm$.00)
NSGA II	9.62 ($\pm$.35)	—	99.26 ($\pm$.80)	11.12 ($\pm$.77)
SMPSO	10.04 ($\pm$.40)	—	105.82 ($\pm$.43)	4.14 ($\pm$.28)

provide even more complex instances. A good performance of existing algorithms in higher dimensional spaces might be a subject for future research.

We want to point out that the generalization of the DMP allows not only to use any metric as a distance measurement, but also non-metric distance relations. The effects on the Pareto-fronts and the behaviour of algorithms when using other distance functions than the ones proposed here might also be of interest for further research.

REFERENCES

[1] H. Ishibuchi, M. Yamane, N. Akedo, and Y. Nojima, "Many-objective and many-variable test problems for visual examination of multiobjective search," in *Evolutionary Computation (CEC), 2013 IEEE Congress on*, 2013, pp. 1491–1498.

[2] R. C. Purshouse and P. J. Fleming, "Evolutionary many-objective optimisation: An exploratory analysis," in *Evolutionary Computation, 2003. CEC'03. The 2003 Congress on*, vol. 3. IEEE, 2003, pp. 2066–2073.

[3] E. Zitzler, K. Deb, and L. Thiele, "Comparison of multiobjective evolutionary algorithms: Empirical results," *Evol. Comput.*, vol. 8, no. 2, pp. 173–195, Jun. 2000. [Online]. Available: http://dx.doi.org/10.1162/106365600568202

[4] K. Deb, L. Thiele, M. Laumanns, and E. Zitzler, "Scalable multi-objective optimization test problems," in *Evolutionary Computation, 2002. CEC '02. Proceedings of the 2002 Congress on*, vol. 1, 2002, pp. 825–830.

[5] S. Huband, L. Barone, L. While, and P. Hingston, "A scalable multi-objective test problem toolkit," in *Evolutionary Multi-Criterion Optimization*, ser. Lecture Notes in Computer Science, C. Coello Coello, A. Hernndez Aguirre, and E. Zitzler, Eds. Springer Berlin Heidelberg, 2005, vol. 3410, pp. 280–295. [Online]. Available: http://dx.doi.org/10.1007/978-3-540-31880-4_20

[6] M. Köppen and K. Yoshida, "Many-objective particle swarm optimization by gradual leader selection," in *Adaptive and Natural Computing Algorithms*. Springer, 2007, pp. 323–331.

[7] ——, "Substitute distance assignments in nsga-ii for handling many-objective optimization problems," in *Evolutionary Multi-Criterion Optimization*. Springer, 2007, pp. 727–741.

[8] O. Schütze, A. Lara, and C. A. Coello Coello, "On the influence of the number of objectives on the hardness of a multiobjective optimization problem," *Evolutionary Computation, IEEE Transactions on*, vol. 15, no. 4, pp. 444–455, 2011.

[9] H. Ishibuchi, Y. Hitotsuyanagi, N. Tsukamoto, and Y. Nojima, "Many-objective test problems to visually examine the behavior of multiobjective evolution in a decision space," in *Parallel Problem Solving from Nature, PPSN XI*. Springer, 2010, pp. 91–100.

[10] H. Ishibuchi, N. Akedo, and Y. Nojima, "A many-objective test problem for visually examining diversity maintenance behavior in a decision space," in *Proceedings of the 13th annual conference on Genetic and evolutionary computation*. ACM, 2011, pp. 649–656.

[11] H. Masuda, Y. Nojima, and H. Ishibuchi, "Visual examination of the behavior of emo algorithms for many-objective optimization with many decision variables," in *Evolutionary Computation (CEC), 2014 IEEE Congress on*, July 2014, pp. 2633–2640.

[12] H. Zille, "Cooperative coevolution for large-scale multiobjective distance minimization problems," Master's thesis, Karlsruhe Institute of Technology (KIT), 2014.

[13] Q. Zhang and H. Li, "Moea/d: A multiobjective evolutionary algorithm based on decomposition," *Evolutionary Computation, IEEE Transactions on*, vol. 11, no. 6, pp. 712–731, 2007.

[14] K. Deb, A. Pratap, S. Agarwal, and T. Meyarivan, "A fast and elitist multiobjective genetic algorithm: Nsga-ii," *Evolutionary Computation, IEEE Transactions on*, vol. 6, no. 2, pp. 182–197, 2002.

[15] A. J. Nebro, J. Durillo, J. Garcia-Nieto, C. Coello Coello, F. Luna, and E. Alba, "Smpso: A new pso-based metaheuristic for multi-objective optimization," in *Computational intelligence in miulti-criteria decision-making, 2009. mcdm'09. ieee symposium on*. IEEE, 2009, pp. 66–73.

[16] K. Deb, *Multi-objective optimization using evolutionary algorithms*, paperback ed., 1. publ. ed., ser. Wiley paperback series. Chichester: Wiley, 2008. [Online]. Available: http://swbplus.bsz-bw.de/bsz309213304cov.htm